

ROM SAF Report 32

An initial assessment of the quality of RO data from KOMPSAT-5

N E Bowler

Met Office, Exeter, UK

Document Author Table

	<i>Name</i>	<i>Function</i>	<i>Date</i>	<i>Comments</i>
Prepared by:	N E Bowler	ROM SAF Project Team	28 Jun 2018	
Reviewed by:	John Eyre	Met Office review	02 Jul 2018	
Reviewed by:	Mary Forsythe	Met Office review	30 Jul 2018	
Reviewed by:	C Piccolo	Met Office approval	02 Aug 2018	
Reviewed by:	S Healy	ROM SAF review	12 Sep 2018	
Approved by:	K B Lauritsen	ROM SAF Project Manager	12 Sep 2018	

Document Change Record

<i>Issue/Revision</i>	<i>Date</i>	<i>By</i>	<i>Description</i>
0.1	28 Jun 2018	NEB	1st draft
1.0	14 Sep 2018	NEB	Final version, following review by ROM SAF PM

ROM SAF

The Radio Occultation Meteorology Satellite Application Facility (ROM SAF) is a decentralised processing centre under EUMETSAT which is responsible for operational processing of GRAS radio occultation (RO) data from the Metop satellites and RO data from other missions. The ROM SAF delivers bending angle, refractivity, temperature, pressure, and humidity profiles in near-real time and offline for NWP and climate users. The offline profiles are further processed into climate products consisting of gridded monthly zonal means of bending angle, refractivity, temperature, humidity, and geopotential heights together with error descriptions.

The ROM SAF also maintains the Radio Occultation Processing Package (ROPP) which contains software modules that will aid users wishing to process, quality-control and assimilate radio occultation data from any radio occultation mission into NWP and other models.

The ROM SAF Leading Entity is the Danish Meteorological Institute (DMI), with Cooperating Entities: i) European Centre for Medium-Range Weather Forecasts (ECMWF) in Reading, United Kingdom, ii) Institut D’Estudis Espacials de Catalunya (IEEC) in Barcelona, Spain, and iii) Met Office in Exeter, United Kingdom. To get access to our products or to read more about the project please go to: <http://www.romsaf.org>

Intellectual Property Rights

All intellectual property rights of the ROM SAF products belong to EUMETSAT. The use of these products is granted to every interested user, free of charge. If you wish to use these products, EUMETSAT’s copyright credit must be shown by displaying the words "copyright (year) EUMETSAT" on each of the products used.

Abstract

The KOMPSAT-5 satellite was launched in 2013 into a sun-synchronous polar orbit. Recently UCAR have started processing the RO data which was being produced by this satellite. These data are made available via FTP from the CDAAC website. The observations are processed twice per day, with a delay of a few hours, which means that they are not currently suitable for operational implementation.

Overall the quality of this data is excellent — approximately as good as from the COSMIC-1 satellites. There is no evidence of systematic biases in the data. The standard deviation of differences between the observation and NWP model background is generally comparable to that of other satellites, except in the lower-stratosphere where they are slightly larger. Due to the orbital period the satellite produces occultations in a regular pattern across the globe. In the one-month period considered we received 12901 observations (approx 440 per day) which compares with 16874 for Metop-A and 7956 for COSMIC-1 FM1.

Contents

1 Bending angle evaluation	5
1.1 Bias and standard deviation characteristics	5
1.2 Vertical correlations	5
2 Refractivity assessment	10
3 Other notable features	13
4 Conclusion	16

1 Bending angle evaluation

1.1 Bias and standard deviation characteristics

Figure 1.1 shows the normalised difference between the bending angle observation and the background forecast from the Met Office’s operational NWP model. The mean and standard deviation are calculated as

$$\mu = \frac{1}{N} \sum_{i=1}^N \frac{O_i - B_i}{B_i} \quad (1.1)$$

$$\sigma = \sqrt{\frac{1}{N} \sum_{i=1}^N \left(\frac{O_i - B_i}{B_i} - \mu \right)^2} \quad (1.2)$$

where O_i and B_i are the observed and background values for occultation i in the period, and there are N occultations overall. The data are from a period of March 2018. From Figure 1.1 we can see that the bias and standard deviation characteristics of data from KOMPSAT-5 are very similar to those from COSMIC-1 FM1 (listed as COSMIC-1). There is a slight negative bias to the bending angles in the troposphere, which is not present in the COSMIC data. This compares with a large positive bias in the tropospheric data for Metop-A. Above the troposphere the biases for the three satellites are remarkably similar, indicating good performance for the KOMPSAT-5 satellite.

The dashed lines in Figure 1.1 show the standard deviation of the normalised observation departures for each satellite. The values are rather similar between all three satellites, with standard deviations slightly less than 2% between around 10km and 35km. The principal difference is that the KOMPSAT data has an increase in standard deviations at around 12km and 18km. The peak at 18km is present in the other data, but is generally smaller, and believed to be due to atmospheric variability caused by gravity-wave breaking in the tropical lower-stratosphere.

Figure 1.2 shows the bias and standard deviation, as Figure 1.1, but separated by different latitude ranges. The increase in standard deviation in the tropical lower-stratosphere is larger for KOMPSAT-5 than for the other two satellites. The other satellites also display an increase in standard deviations at around 10km for high latitudes. However, for KOMPSAT-5 there is a much larger increase in the standard deviation, and this occurs at a slightly larger impact height. These results suggest that the two increases in standard deviation seen in Figure 1.1 are due to similar causes — related to the behaviour of the observation in the lower-stratosphere at different latitudes.

1.2 Vertical correlations

When bending angle data is assimilated into the Met Office’s DA system it is assumed that the error in each bending angle measurement is independent of the errors in every other measurement. Therefore we would like vertical correlations of $O - B$ to be close to diagonal. Figure 1.3 shows the vertical correlation of the normalised difference between the observation and NWP model background forecast. Due to the way that bending angle is calculated as a smoothed difference between Doppler shifts, we expect a region of positive correlations near the diagonal, and negative correlations at further distances. The data from KOMPSAT is very similar to that from COSMIC-1. The only clear exception to this is an increase in the correlation width around 12km impact height. It is noticeable

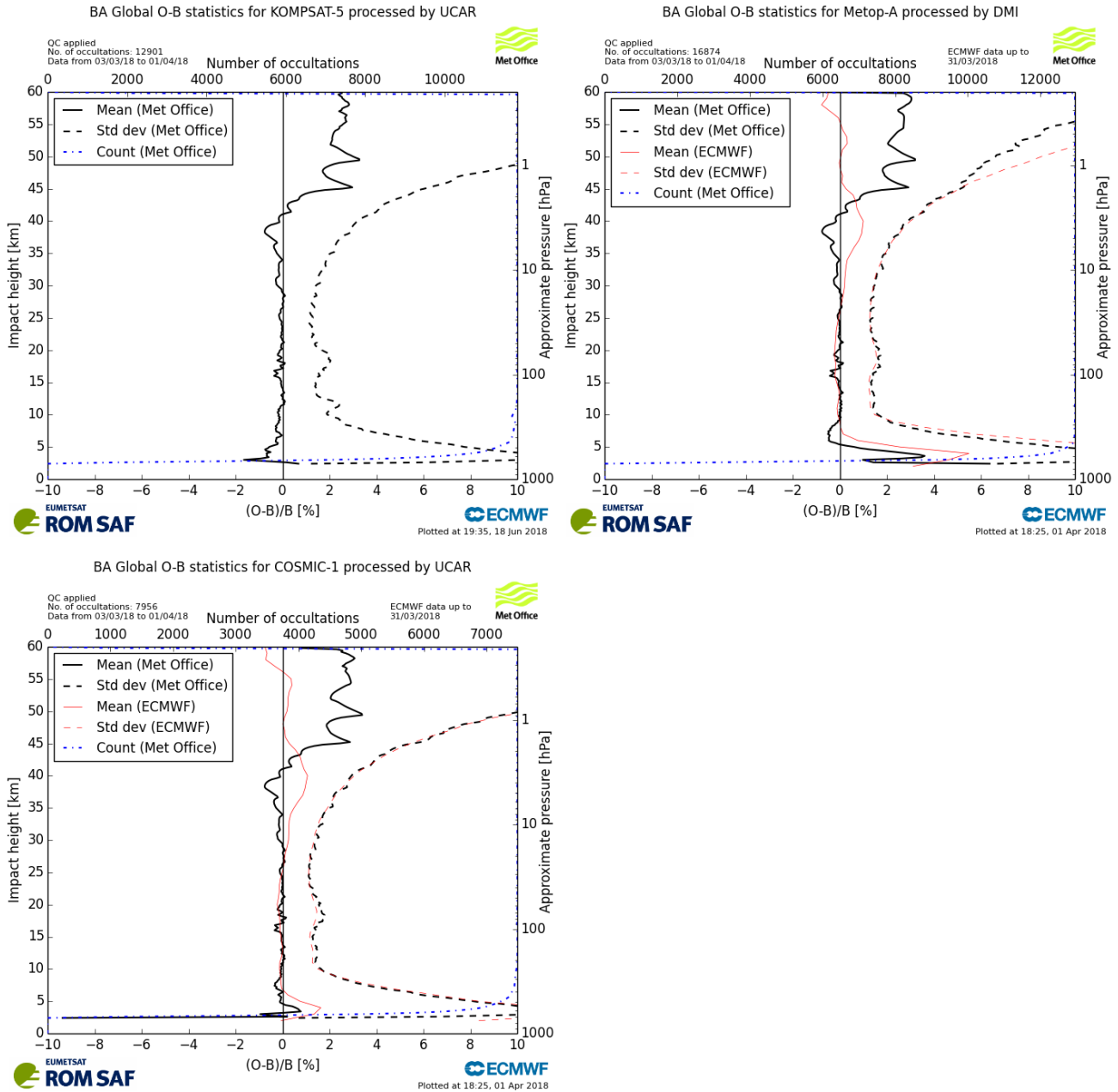


Figure 1.1: The bias and standard deviation of the normalised difference between the observation and the NWP model background forecast $(O - B)/B$ for bending angle.

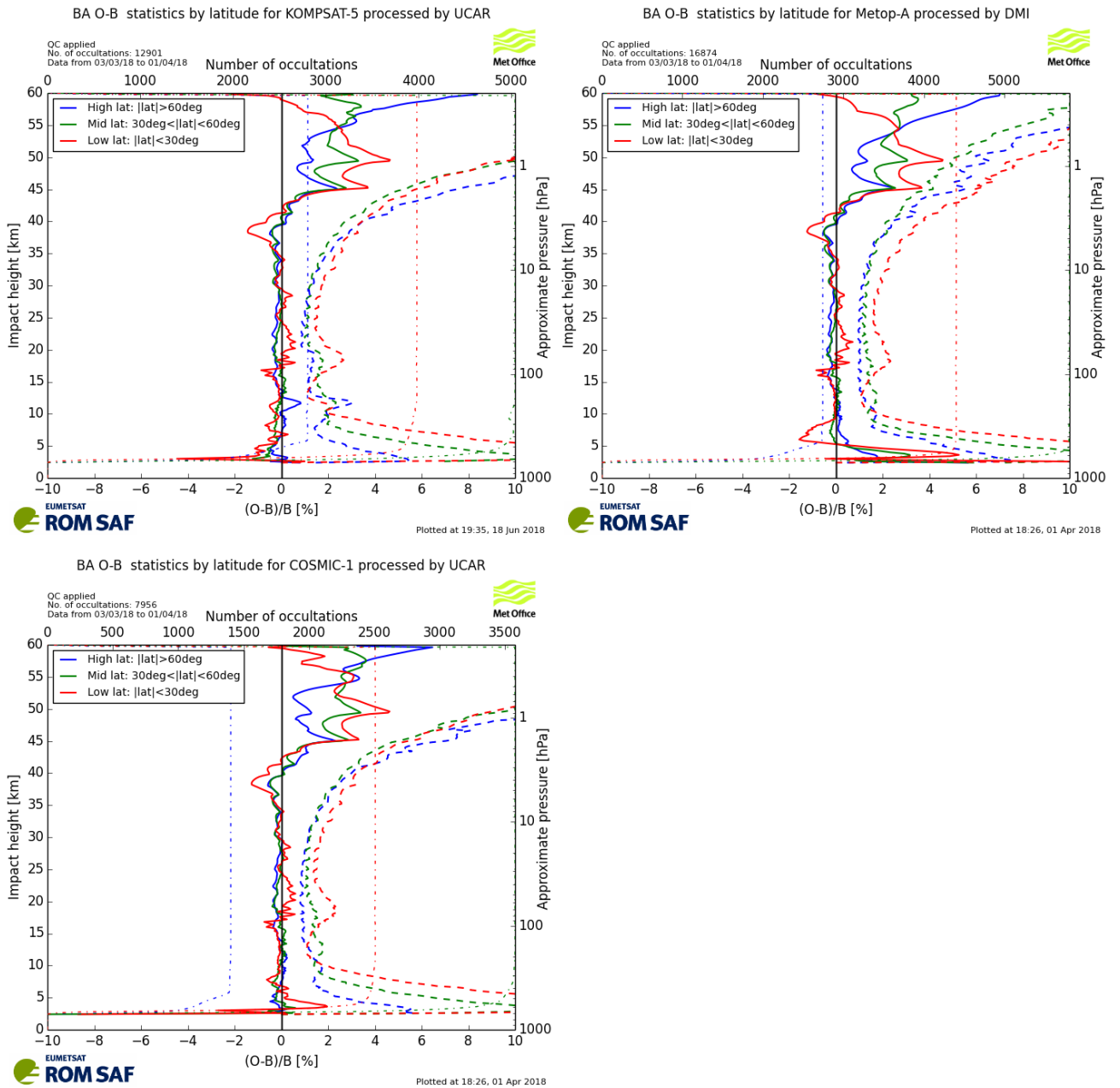


Figure 1.2: The bias and standard deviation of the normalised difference between the observation and the NWP model background forecast $(O - B)/B$, separated by different latitudes for bending angle.

that long-range positive correlations above 30km are present in both KOMPSAT-5 and COSMIC-1 data, but absent in that for Metop-A. Metop-A also has longer-range vertical correlations in the troposphere than the other two satellites.

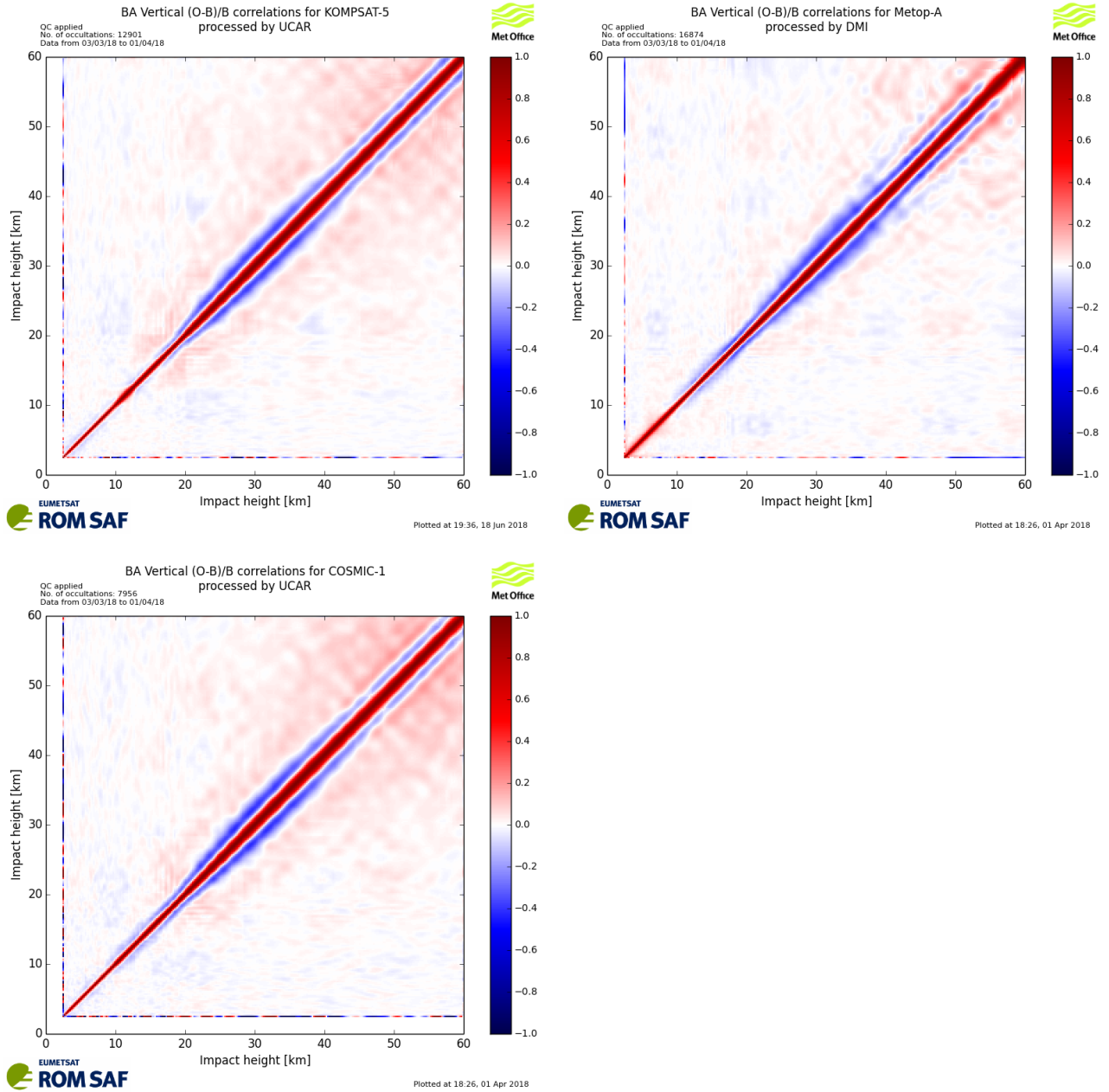


Figure 1.3: Vertical correlations of normalised differences between the observation and the NWP model background for bending angle.

2 Refractivity assessment

The performance of refractivity observations is similar to the bending angle performance. Therefore, this will only be discussed briefly. Figure 2.1 shows the mean and standard deviation of normalised differences between the observed refractivity and that produced by the NWP model forecast. The KOMPSAT-5 data is very similar to that from COSMIC-1. There is a small signal of increased standard deviations at 18km and 12km. The issues at these levels are more visible in the vertical correlation plot (Figure 2.2).

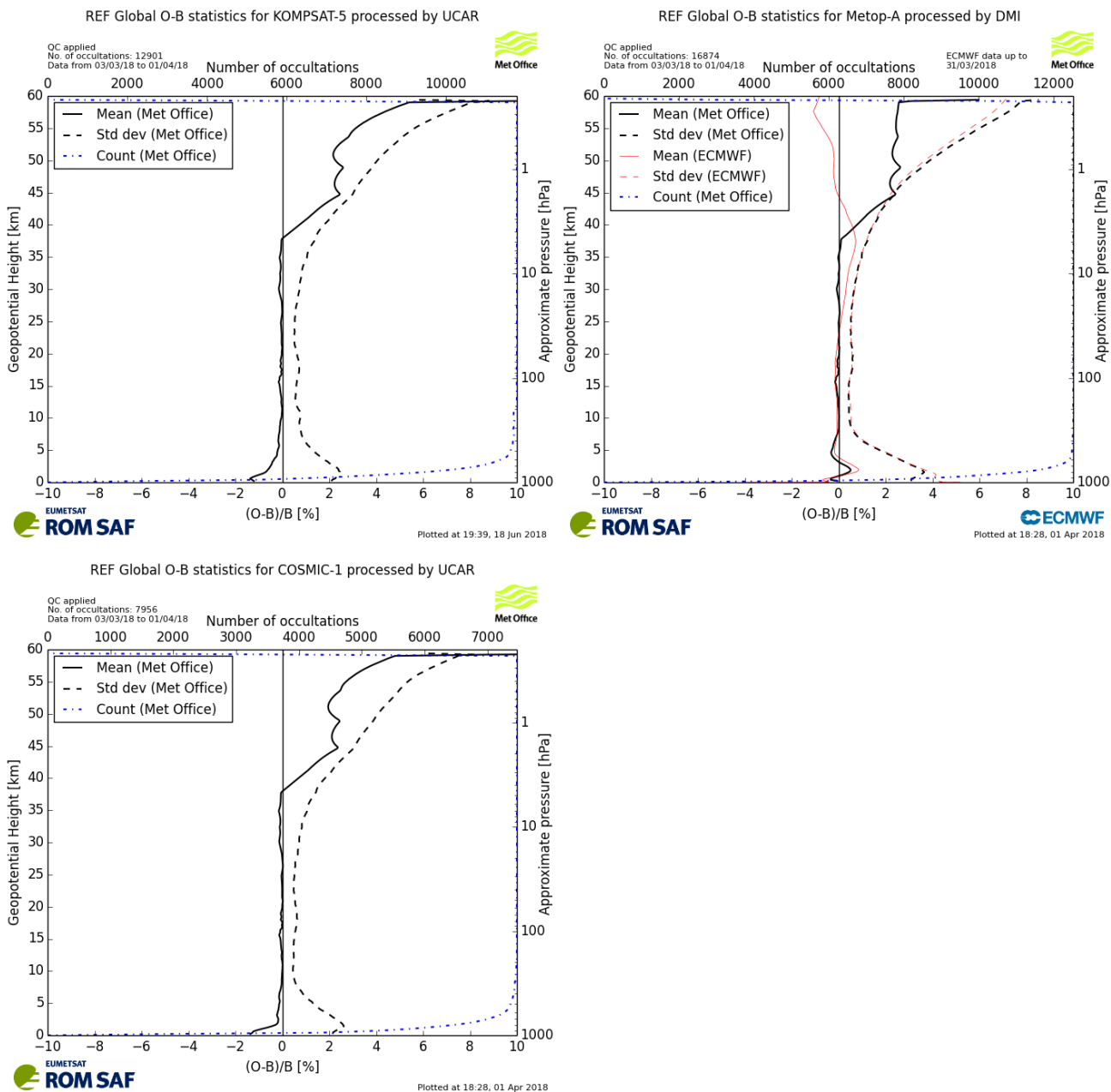


Figure 2.1: The bias and standard deviation of the normalised difference between the observation and the NWP model background forecast $(O - B)/B$ for refractivity.

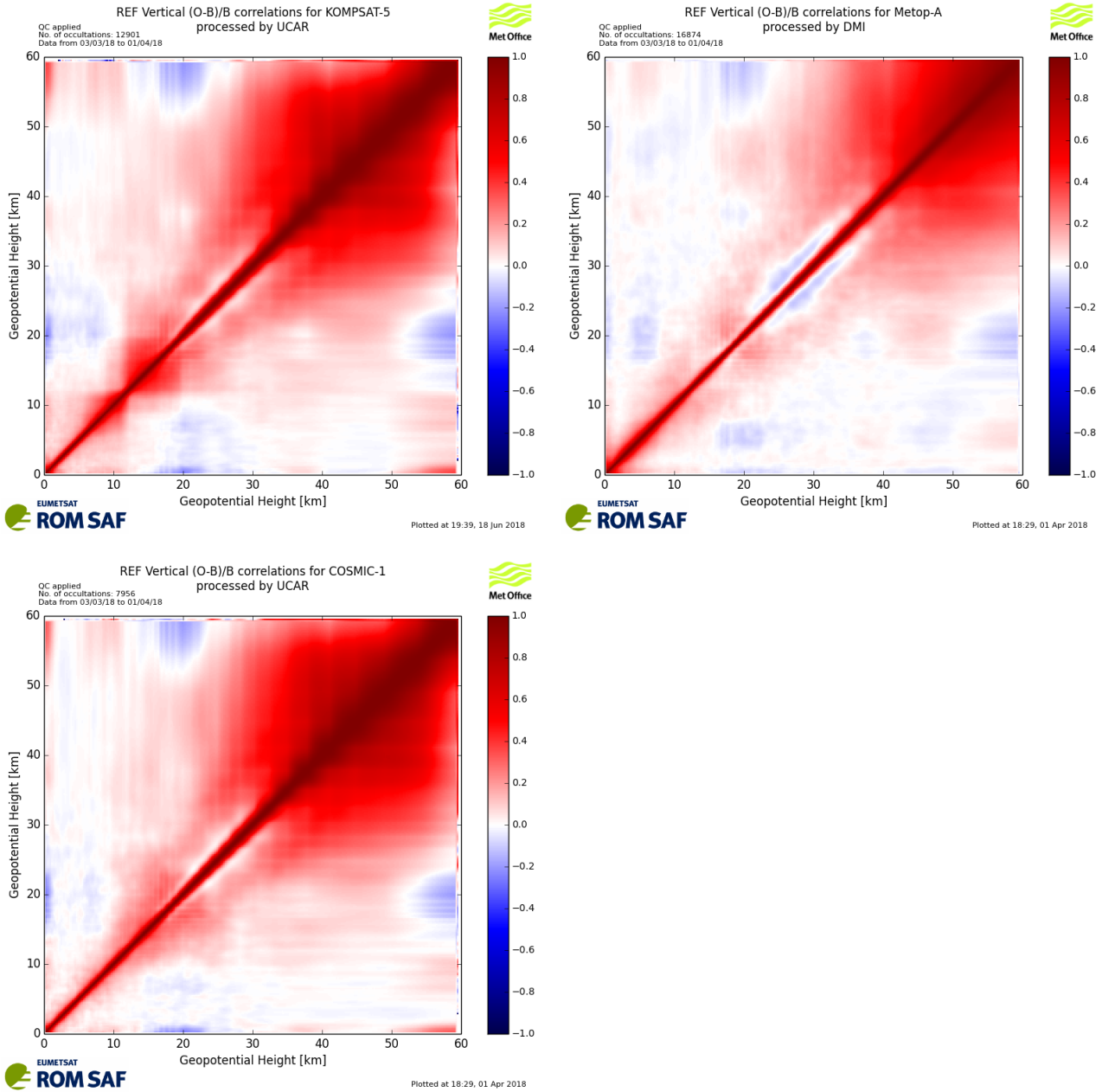


Figure 2.2: Vertical correlations of normalised differences between the observation and the NWP model background for refractivity.

3 Other notable features

KOMPSAT-5 is in a sun-synchronous orbit at an altitude of around 550km. This means that it completes 15 1/28 orbits of the earth each day. Therefore it is passing over the same location on earth every 23 hours and 57 minutes (approximately). This is approximately the time it takes the GPS satellites to perform two orbits. Therefore occultations occur in nearly the same place on consecutive days. Figure 3.1 shows the locations of occultations for KOMPSAT-5 over March 2018. This regular pattern is not seen for other satellites.

On a separate note, this assessment was based on data from March 2018. Initially a period of May 2017 was analysed. Although the quality was very similar to that presented here the PCD flag indicating whether the occultation was rising or setting was not set. Therefore the software assumed that all occultations were setting. This flag is ignored by the Met Office's data assimilation system, so its absence from the earlier period is troubling, but not a critical issue. The changeover to start including the rising/setting flag is in early December 2017

The data is not currently being processed in real time. Judging by the time-stamps on the occultation files the processing takes place twice per day, on data which is a few hours old. Therefore the time delay in processing a given occultation is many hours, as is shown in Figure 3.2. We would normally seek to receive observations within three hours for these to be used in operational assimilation.

BA Occultation locations for KOMPSAT-5 processed by UCAR

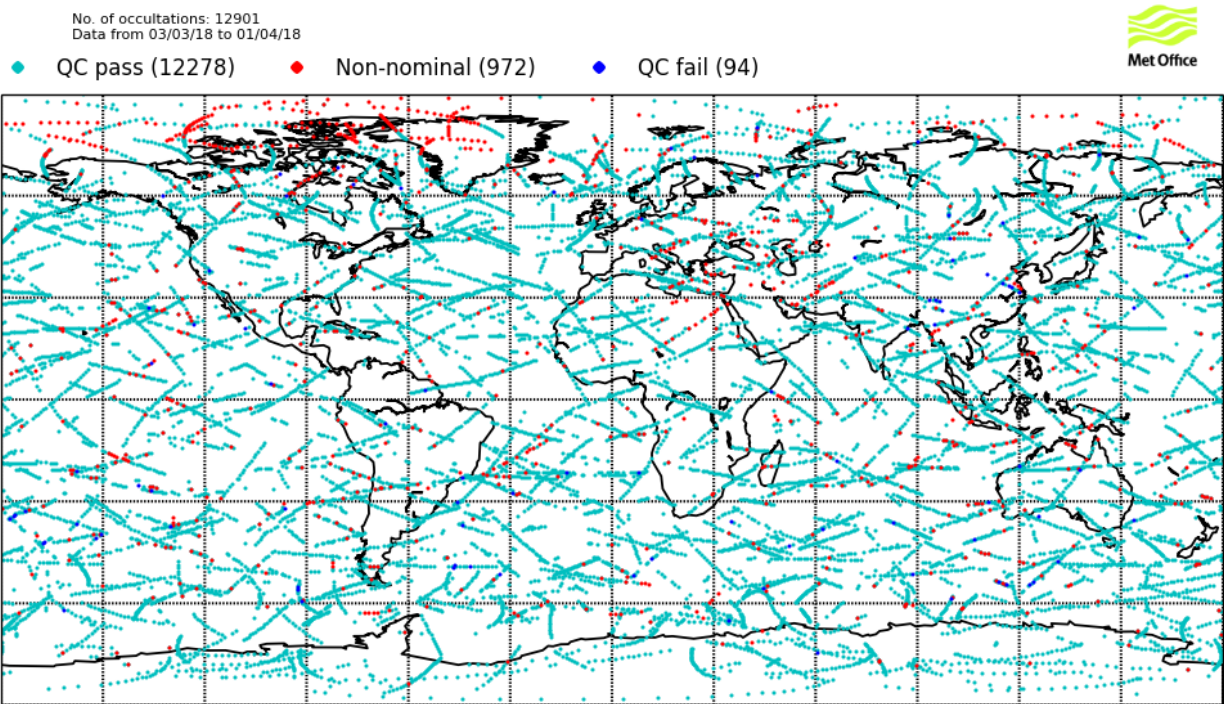


Figure 3.1: Location of the occultations for KOMPSAT-5 over a 1 month period.

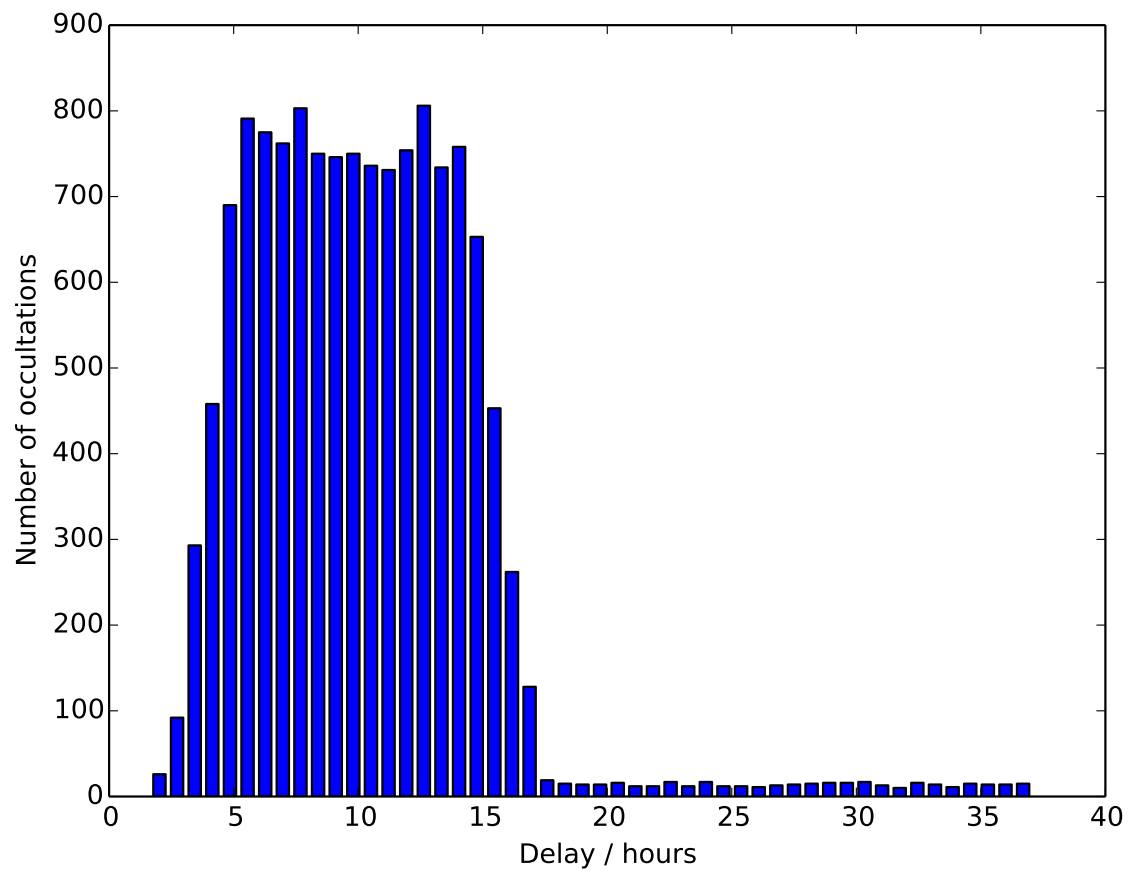


Figure 3.2: Time delay in processing the occultations, as calculated from the time-stamp of the files.

4 Conclusion

Given that the overall quality of these observations appear to be very good, the next logical step would to run an NWP trial assimilating these observations. If that trial performs well, then it would be desirable to use these data operationally, provided that they can be produced and disseminated in a timely fashion.

ROM SAF (and earlier GRAS SAF) Reports

SAF/GRAS/METO/REP/GSR/001	Mono-dimensional thinning for GPS Radio Occultation
SAF/GRAS/METO/REP/GSR/002	Geodesy calculations in ROPP
SAF/GRAS/METO/REP/GSR/003	ROPP minimiser - minROPP
SAF/GRAS/METO/REP/GSR/004	Error function calculation in ROPP
SAF/GRAS/METO/REP/GSR/005	Refractivity calculations in ROPP
SAF/GRAS/METO/REP/GSR/006	Levenberg-Marquardt minimisation in ROPP
SAF/GRAS/METO/REP/GSR/007	Abel integral calculations in ROPP
SAF/GRAS/METO/REP/GSR/008	ROPP thinner algorithm
SAF/GRAS/METO/REP/GSR/009	Refractivity coefficients used in the assimilation of GPS radio occultation measurements
SAF/GRAS/METO/REP/GSR/010	Latitudinal Binning and Area-Weighted Averaging of Irregularly Distributed Radio Occultation Data
SAF/GRAS/METO/REP/GSR/011	ROPP 1dVar validation
SAF/GRAS/METO/REP/GSR/012	Assimilation of Global Positioning System Radio Occultation Data in the ECMWF ERA-Interim Re-analysis
SAF/GRAS/METO/REP/GSR/013	ROPP PP validation
SAF/ROM/METO/REP/RSR/014	A review of the geodesy calculations in ROPP
SAF/ROM/METO/REP/RSR/015	Improvements to the ROPP refractivity and bending angle operators
SAF/ROM/METO/REP/RSR/016	Simplifying EGM96 undulation calculations in ROPP
SAF/ROM/METO/REP/RSR/017	Simulation of L1 and L2 bending angles with a model ionosphere
SAF/ROM/METO/REP/RSR/018	Single Frequency Radio Occultation Retrievals: Impact on Numerical Weather Prediction
SAF/ROM/METO/REP/RSR/019	Implementation of the ROPP two-dimensional bending angle observation operator in an NWP system
SAF/ROM/METO/REP/RSR/020	Interpolation artefact in ECMWF monthly standard deviation plots
SAF/ROM/METO/REP/RSR/021	5th ROM SAF User Workshop on Applications of GPS radio occultation measurements
SAF/ROM/METO/REP/RSR/022	The use of the GPS radio occultation reflection flag for NWP applications
SAF/ROM/METO/REP/RSR/023	Assessment of a potential reflection flag product
SAF/ROM/METO/REP/RSR/024	The calculation of planetary boundary layer heights in ROPP
SAF/ROM/METO/REP/RSR/025	Survey on user requirements for potential ionospheric products from EPS-SG radio occultation measurements

ROM SAF (and earlier GRAS SAF) Reports (cont.)

SAF/ROM/METO/REP/RSR/026	Estimates of GNSS radio occultation bending angle and refractivity error statistics
SAF/ROM/METO/REP/RSR/027	Recent forecast impact experiments with GPS radio occultation measurements
SAF/ROM/METO/REP/RSR/028	Description of wave optics modelling in ROPP-9 and suggested improvements for ROPP-9.1
SAF/ROM/METO/REP/RSR/029	Testing reprocessed GPS radio occultation datasets in a reanalysis system
SAF/ROM/METO/REP/RSR/030	A first look at the feasibility of assimilating single and dual frequency bending angles

ROM SAF Reports are accessible via the ROM SAF website: <http://www.romsaf.org>